Lattice dynamics of $Fe_{0.5}Ti_{0.5}$

U. Buchenau, H. R. Schober, J.-M. Welter, G. Arnold, and R. Wagner
Institut für Festkörperforschung, Kernforschungsanlage Jülich, 5170 Jülich, West Germany
(Received 19 March 1982)

The phonon dispersion curves for the intermetallic compound $Fe_{0.5}Ti_{0.5}$ at room temperature have been determined by inelastic neutron scattering. The initial slopes of the dispersion curves at low frequencies were measured with a triple-axis spectrometer with the use of a small single crystal. The resulting elastic constants are $c_{11}=325\pm10$ GPa, $c_{12}=121\pm10$ GPa, and $c_{44}=69\pm1$ GPa. The phonons at higher frequencies were determined by fitting Born–von Kármán force constants to time-of-flight spectra obtained from a polycrystalline sample. A good reproduction of the measured intensities could be obtained with tensor force constants between atoms up to the fourth neighbors. A striking feature of the result is the strong Ti-Ti nearest-neighbor longitudinal force constant which is about twice as strong as the corresponding Fe-Fe one. The averaged force constants correspond closely to the values found in chromium, which has very similar electronic structure.

I. INTRODUCTION

$Fe_{0.5}Ti_{0.5}$ is not only a promising hydrogen storage material[1] but an interesting intermetallic compound in its own right. It is isoelectronic with chromium, having an average of six valence electrons per atom. It has the CsCl structure with a lattice constant $a=2.977$ Å at room temperature and remains ordered up to its formation temperature of 1590 K. Its electronic structure bears a close resemblance to the electronic structure of chromium, though of course the different electronic configurations of Fe and Ti lead to a stronger association of the occupied d states with the Fe sites.[2–4] These similarities and differences between the two substances $Fe_{0.5}Te_{0.5}$ and chromium should be reflected in the phonon dispersion. In this work we report measurements of the phonons in $Fe_{0.5}Ti_{0.5}$ by inelastic neutron scattering. Two different techniques were used. At low frequencies (below 2 THz) phonons were measured in the usual way with a small single crystal on a triple-axis spectrometer. Thus elastic constants could be determined. At higher frequencies a new technique[5] was employed, which allows the determination of a set of lattice dynamical parameters from the time-of-flight spectrum scattered from a polycrystalline sample. The details of the elastic constant determination including the sample preparation will be given in Sec. II. Section III deals with the determination of the full phonon dispersion from the time-of-flight data. Section IV contains the results and their discussion, the comparison with chromium, and calculated results for the phonon density of states and the specific heat.

II. SAMPLE PREPARATION AND DETERMINATION OF ELASTIC CONSTANTS

The compound was formed by rf-induction melting of the elements in a horizontal boat crucible and was homogenized by levitation melting. The starting materials were zone-melted titanium (99.98% pure) from Materials Research Corp. and sintered iron sponge (99.998% pure) from Johnson Matthey Chemicals Ltd. Water-cooled copper crucibles and high-purity argon atmospheres were used. Powder samples were prepared by crushing the knob obtained after levitation in a mortar. Single crystals were grown with a floating-zone technique. The starting rods were cast in an arc melter which is equipped with a suction crucible. Further details on the preparation, machining, and characterization of high-quality $Fe_{0.5}Ti_{0.5}$ samples are found in Ref. 6.

The sample used for the determination of the elastic constants was a single crystal with a diameter of ~5 mm and a length of ~18 mm, yielding a volume of ~350 mm^3. Its mosaic width was about 1.2°. With a crystal of this size it is easy to determine phonons below 2 THz, even for a hard substance. The phonons were measured on the triple-axis spectrometer SV4 in the reactor DIDO in Jülich. Pyrolytic graphite crystals [(002)reflection]

were used in the double monochromator and as analyzer. The collimation sequence was 120'-45'-45'-45'. The transverse phonons were measured in both energy gain and energy loss, the longitudinal ones only in energy loss of the sample.

The initial slopes of the phonon branches which can be determined from the phonon frequencies reported in Table I give the wave velocities $v=\sqrt{c/\rho}$, where ρ is the mass density and c corresponds to c_{11}, $c'=(c_{11}-c_{12})/2$, or c_{44} for the three phonon branches of Table I, respectively. With $\rho=6.53\times10^3$ kg/m^3, one obtains the elastic constants shown in the first column of Table II.

With an ultrasonic method the two wave velocities $v_L(110)$ and $v_L(111)$ were measured by Fisher[7] (Argonne National Laboratory) at room temperature on a thin monocrystalline disc with (110) faces. He obtained the elastic coefficient c_{11} and with limited accuracy $c'-c_{44}$. The values are listed in Table II. By gravimetric weighting in CCl_4 the density of the sample was determined to be 6.488×10^3 kg/m^3 which is only 0.6% less than the x-ray value. The coefficient c_{11} agrees surprisingly well with the one determined by neutron spectroscopy. One should expect that the neutron data should be 5 to 10% higher. The reason is that here the crystal is probed in the THz range, whereas in ultrasonic work a MHz range is used where relaxation effects are more pronounced. This could explain the slightly lower value found ultrasonically by Liebertz *et al.*[8] for the c_{11} coefficient at 293 K. It is not clear whether the larger discrepancies for the c_{12} and c_{44} coefficients are due to a different range of excitation frequencies or to difficulties in measuring transverse modes accurately. The crystal used by Liebertz *et al.* was grown in a graphite crucible and therefore the pickup of carbon could lead to carbide inhomogeneities in the lattice.

III. TIME-OF-FLIGHT MEASUREMENTS

A. Method

The phonon dispersion curves at higher frequencies were determined from the inelastic neutron scattering from a polycrystalline $Fe_{0.5}Ti_{0.5}$ sample. The scattering from a polycrystal corresponds to a suitably weighted orientation average of the scattering from a single crystal. For a completely random distribution of orientations of the crystallites, the scattering depends only on the energy transfer $h\nu$ and the absolute value Q of the momentum transfer and is independent of the direction of $\vec{Q}$. For the incoherent part of the scattering, there is no selection rule with respect to the momentum transfer and the resulting intensities reflect merely the phonon density of states.[9] Most elements, however, have strong coherent cross sections. For coherent scatterers, the momentum selection rule $\vec{Q}=\vec{G}+\vec{q}$ ($\vec{G}$ reciprocal-lattice point, $\vec{q}$ phonon wave vector) for the one-phonon scattering process introduces additional structure along lines of constant frequency ν and consequently additional information. Though this information is clearly less than the information obtainable from a single crystal, still a limited number of lattice-dynamical parameters may be obtained by fitting the polycrystal scattering.

The method has been tested successfully for polycrystalline aluminum yielding an average accuracy of 2–3% for the phonon frequencies.[5] It has been used to determine the phonon dispersion curves of fcc calcium at room temperature. The dispersion curves of calcium were not known, because it is extremely difficult to bring a single crystal through the bcc-fcc transition at 720 K in this material. Nevertheless, the task of growing a suitable single crystal was achieved very recently by a group at the Ames Laboratory. The phonons measured at Oak Ridge National Laboratory using this crystal[10] agree within 3–6% with those determined from the polycrystal.[5]

The applicablility of the method to crystals with two atoms per unit cell has been tested using a polycrystalline KBr sample. The resulting phonon frequencies again showed excellent agreement with single-crystal results.[11] The deviations were of the order of only a few percent both for the acoustic- and the optical-phonon branches. From a methodical point of view, $Fe_{0.5}Ti_{0.5}$ has the disadvantage of having two atoms with only a small difference in

TABLE I. Low-frequency phonons in $Fe_{0.5}Ti_{0.5}$.

$\|00\zeta\|L$		$\|00\zeta\|T$		$\|0\zeta\zeta\|T_2$	
ζ $(2\pi/a)$	ν (THz)	ζ $(2\pi/a)$	ν (THz)	ζ $(2\pi/a)$	ν (THz)
0.045	1.05±0.02	0.1	1.06±0.01	0.06	1.1 ±0.1
0.06	1.43±0.03	0.12	1.33±0.01	0.08	1.51±0.06

TABLE II. Elastic constants of $Fe_{0.5}Ti_{0.5}$ in GPa.

	This work (neutrons)	Fisher (Ref. 7) (ultrasonics)	Liebertz *et al.* (Ref. 8) (ultrasonics)
c_{11}	325±10	323.3	310±2
c_{12}	121±10		86.2±4
c_{44}	69±1		74.9±1
$c'-c_{44}$	33±8	46.8	37

mass, so no clear separation of acoustic- and optic-phonon branches as in KBr can be expected. It has the advantage of opposite sign and unequal absolute values of the scattering lengths, which should give distinguishable contributions of the two atoms to the scattering. It has the further advantage that from the analogy to chromium one might expect to be able to describe the phonon dispersion with a relatively small number of force constants (chromium can be described satisfactorily with force constants up to the fourth neighbors[12]). Thus a reasonable number of parameters can be used and it should be possible to check the force-constant fit obtained from the polycrystal by the elastic constants obtained from the small single crystal.

In order to fit force constants to the polycrystal scattering, one starts with a plausible force-constant set and calculates phonon frequencies $\nu_j(\vec{q})$ ($j=1,2,\ldots,3r$ for r atoms in the unit cell) and phonon eigenvectors $e_d^j(\vec{q})$ ($d=1,\ldots,r$) for all phonon wave vectors $\vec{q}$ on a fine mesh of points in the Brillouin zone. The mesh divides the reciprocal space into small cubes of volume d^3q centered around the points. The phonon frequencies and eigenvectors are assumed to be constant within one cube. For cubic substances only $\frac{1}{48}$ of the whole Brillouin zone need be considered. The intensity calculations are based on the textbook formulas for the coherent[13] and incoherent[14] one-phonon scattering cross sections for a single crystal. In order to simplify the expressions, let us consider only one given phonon, one given reciprocal-lattice point $\vec{G}$, and only the phonon annihilation process (the phonon creation is completely analogous). Then the coherent scattering cross section[13] reduces to

$$\left[\frac{d^2\sigma(\mathrm{coh})}{d\Omega d\nu}\right]_{\mathrm{cryst}}^{\text{1-ph}}=\frac{2\hbar k_f\pi^2}{k_i V_0}\frac{|F_j(\vec{Q},\vec{q})|^2}{\nu_j(\vec{q})}n_j(q)\delta(\nu+\nu_j(\vec{q}))\delta(\vec{Q}-(\vec{G}-\vec{q})) \tag{1}$$

with the structure factor

$$F_j(\vec{Q},\vec{q})=\sum_d \bar{b}_d e^{-W_d(\vec{Q})}e^{i\vec{Q}\cdot\vec{d}}[\vec{Q}\cdot\vec{e}_d^{\,j}(\vec{q})]M_d^{-1/2}\,, \tag{2}$$

where Ω denotes the solid angle, k_f and k_i are the absolute values of the final and the initial wave vectors of the neutron, V_0 is the volume of the unit cell, $n_j(\vec{q})$ is the thermal population of the phonon, $\vec{d}$ is the position of the dth atom with respect to the origin of the unit cell, M_d is its mass, $\bar{b}_d$ its average scattering length, and $-W_d(\vec{Q})$ the exponent of its Debye-Waller factor.

If the variation of the phonon frequency and eigenvector within the small cube is neglected, the intensity contribution of the small cube is simply obtained by multiplying (1) with the volume d^3q and with the density of states in the reciprocal space $NV_0/(2\pi)^3$ (N number of unit cells in the crystal). In order to get the corresponding intensity contribution for a polycrystal with the same total number of unit cells, the momentum δ function must be averaged over all possible crystal orientations[15]:

$$\left[\frac{d^2\sigma(\mathrm{coh})}{d\Omega d\nu}\right]_{\mathrm{poly}}d^3q=\frac{N\hbar k_f}{16\pi^2 k_i(\vec{G}-\vec{q})^2}\frac{|F_j(\vec{G}-\vec{q},\vec{q})|^2}{\nu_j(\vec{q})}n_j(\vec{q})\delta(\nu+\nu_j(\vec{q}))\delta(Q-|\vec{G}-\vec{q}|)d^3q\,. \tag{3}$$

By folding formula (3) with the spectrometer resolution function and summing over j for all $\vec{q}$ values of the mesh and all Brillouin-zone centers $\vec{G}$, one gets the one-phonon annihilaton part of the coherent scattering spectrum of an ideal polycrystal. The determination of the incoherent one-phonon scattering is much easier. For isotropic Debye-Waller factors as in $Fe_{0.5}Ti_{0.5}$ one gets the orientation average of the corresponding single-crystal cross section,[14]

$$\left[\frac{d^2\sigma(\mathrm{inc})}{d\Omega d\nu}\right]_{\mathrm{poly}}d^3q=\frac{NV_0\hbar k_f Q^2}{384\pi^5 k_i\nu_j(\vec{q})}\sum_d\frac{\sigma_{\mathrm{inc}}^d}{M_d}[\vec{e}_d^{\,j}(\vec{q})]^2e^{-2W_d(Q)}n_j(\vec{q})\delta(\nu+\nu_j(\vec{q}))d^3q \tag{4}$$

(σ_{inc}^{d} incoherent scattering cross section of dth atom). Formula (4) folded with the spectrometer resolution and summed over j and $\vec{q}$ gives the incoherent one-phonon annihilation spectrum of an ideal polycrystal.

The calculation of the coherent and incoherent one-phonon scattering for given Born—von Kármán force constants between the atoms allows a comparison between predicted and observed polycrystal scattering intensities. By a suitable procedure, the force constants can be fitted to the measurements.

B. Spectrometer and sample

In order to obtain as much information as possible, it is necessary to measure in a wide range of Q values and over the whole range of lattice frequencies. The suitable spectrometer to measure simultaneously a whole field in Q and ν is the time-of-flight spectrometer. It has the additional advantage of a constant solid angle at all frequencies, which implies that the whole field of intensities can be calibrated with only one spectrometer factor.

The spectrometer SV5 at the reactor DIDO in Jülich was used in this work. Neutrons with a wavelength of 4.78 Å coming from the cold source are selected by a pyrolitic graphite monochromator and chopped by a curved slit chopper situated near the sample. The curved slit chopper suppresses higher orders and produces neutron pulses of a width of 20 μs every 8 ms. 64 detector banks at a distance of 3 m from the sample cover a scattering-angle range from 20° to 160°. The time of arrival of the neutrons at the detectors depends on their velocity and consequently on the energy gained or lost in the scattering processes. Thus one gets a two-dimensional intensity field in scattering angle and time which corresponds to a spectrum in Q and ν.

The sample, 61.3 g of a fine-grained $Fe_{0.5}Ti_{0.5}$ powder (grain size about 50 μm), was filled into a flat thin-walled stainless-steel container of 100-mm height and lateral dimensions of 5×40 mm^2. In order to use the full beam size (100-mm high, 30-mm wide), the container was put into the beam with the flat side at 45° to the beam direction.

The energy of the incoming neutrons corresponded to a frequency of 0.86 THz. This is only a small fraction of the maximum lattice frequency ($\sim$10 THz). Therefore only the phonon annihilation part of the spectrum where the neutrons have gained energy contains the desired information. For the evaluation, the frequency range between 2 and 13 THz was selected (at lower frequencies, the phonons are still nearly exclusively determined by the elastic constants). In a rough approximation the resolution of the spectrometer in time and angle may be assumed to be constant in the whole range and to correspond to the one found for elastically scattered neutrons. Since the energy is not linear in time scale, the energy resolution varied in this approximation from $\sim$0.15 THz at 2 THz to $\sim$0.9 THz at 10 THz. The Q resolution was of the order of 0.04 Å^{-1} in the whole range. The scattering-angle range corresponded to a momentum range of 1.2 to 3.6 Å^{-1} at 2 THz and of 3.4 to 5.8 Å^{-1} at 10 THz. This range covers essentially the first six to seven different Brillouin zones of FeTi in an extended-zone scheme.

C. Calibration and corrections

Before comparing the measured intensities with any calculation based on a lattice-dynamical model one has to calibrate the intensities and to apply a number of corrections: self-absorption correction, subtraction of empty container signal, multiple-scattering correction, and finally multiphonon scattering correction. These corrections are important since the information is contained in the absolute intensities. Fortunately, most of the neutron scattering intensity was due to one-phonon scattering processes. Therefore rather crude approximations for the corrections could be used.

The calibration was done by measuring a time-of-flight spectrum with a weighted small amount of vanadium, which is an incoherent scatterer with a well-known scattering cross section. The scattering lengths used for Fe and Ti were $b_{\text{Fe}}=0.95\times10^{-14}$ m and $b_{\text{Ti}}=-0.34\times10^{-14}$ m, respectively, the incoherent scattering cross sections $\sigma_{\text{inc}}^{\text{Fe}}=0.38\times10^{-28}$ m^2 and $\sigma_{\text{inc}}^{\text{Ti}}=2.75\times10^{-28}$ m^2, the absorption cross sections $\sigma_{\text{abs}}^{\text{Fe}}=2.62\times10^{-28}$ m^2 and $\sigma_{\text{abs}}^{\text{Ti}}=5.8\times10^{-28}$ m^2, the last two values for neutrons of a velocity of 2200 m/s. For the self-absorption correction both absorption and scattering processes have to be considered. The dependence of the elastic scattering cross section on the energy of the scattered neutrons[15] was taken into account explicitly. The flat rectangular sample shape and the position of the sample in the spectrometer make this correction most prominent for detectors near a scattering angle of 45°. After this correction, the empty container signal (measured separately) could be subtracted.

The multiple scattering was relatively weak (only

13% of the incoming neutrons were scattered). Therefore only double scattering was considered. The sequences elastic-inelastic and inelastic-elastic were taken into account by simply augmenting the incoherent scattering cross sections of Fe and Ti used in the program for calculating the theoretical intensities by about 25% of their respective total scattering cross section. The value of 25% resulted from a consideration of the average scattering probabilities for both sequences. The inelastic-inelastic scattering was approximated by first averaging the spectrum for all detectors and then folding this average inelastic spectrum with itself. The multiphonon scattering was calculated in the Gaussian approximation[16] with a Debye temperature of 480 K. After subtracting the last two corrections, the intensities above 10 THz were in fact zero within a reasonable error range for all detectors as they should be for a one-phonon scattering spectrum above the maximum phonon frequency. The corrected spectrum is shown on the left-hand side of Fig. 1.

IV. RESULTS AND DISCUSSION

The experimental data were fitted using a set of Born–von Kármán force constants. In chromium, the phonons are well described by force constants[12] up to the fourth-nearest neighbors (see last column of Table III). An adequate fit of our data requires force constants extending at least to the third neighbors. The fourth neighbors included in the final fit improved the R value (a measure for the quality of the fit) from 5.6% to 4.1%. The right-hand side of Fig. 1 shows the resulting calculated neutron spectrum. The fitted force constants are shown in Table III. The designations of the force constants are as in bcc chromium. These force constants must be duplicated in the CsCl structure for those neighbor pairs which consist of two equal atoms, because Ti-Ti and Fe-Fe pairs have to be considered separately. For the second neighbors (the 200 neighbor in units of $a/2$), the longitudinal force constant is nearly twice as strong for Ti-Ti as for Fe-Fe. The transverse force constant of these pairs is negative for Ti-Ti and positive for Fe-Fe, implying a repulsive force in the first and an attractive force in the second case. In fact Ti seems to have the bigger atomic radius of the two atoms, as evidenced by the lattice constants of the pure substances, by the concentration dependence of the lattice parameter[17] in the monophase region of the compound $Fe_{0.5}Ti_{0.5}$, and by the existence of the Laves phase Fe_2Ti. It should be mentioned that by exchanging the two atoms and fitting again one arrives at a second minimum in the sum of squares which is nearly as low as the first and has practically exchanged force constants. This second minimum was discarded, not only because of the ionic radius argument, but also because the elastic constants calculated from this second set of force constants differed strongly (up to 40%) from the measured ones, while those calculated from the values in Table III show good agreement.

The fourth column in Table III contains averaged force constants which are closely similar to the chromium values in the last column. As pointed out above, these similarities are very probably connected with the similarities in the band structures of the two substances. A deeper discussion of the similarities and differences must await a better understanding of the phonons in metals with d elec-

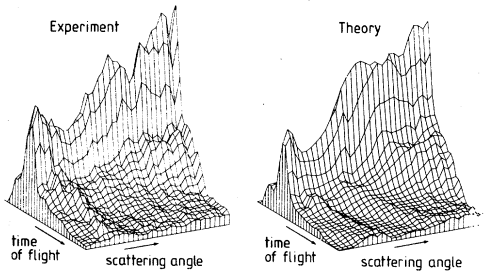

FIG. 1. Experimental (left-hand side) and theoretical (right-hand side) inelastic neutron spectra scattered from polycrystalline $Fe_{0.5}Ti_{0.5}$.

TABLE III. Born–von Kármán parameters of $Fe_{0.5}Ti_{0.5}$ (N/m) determined by coherent neutron scattering from polycrystals at room temperature. Elastic constants (values measured by scattering from single crystals in parentheses): $c_{11}=327$ GPa (325), $c_{12}=126$ GPa (121), $c_{44}=64$ GPa (69).

Neighbor and indices	$Fe_{0.5}Ti_{0.5}$ Ti	$Fe_{0.5}Ti_{0.5}$ Fe	$Fe_{0.5}Ti_{0.5}$ Average	Cr
1xx	12.15±0.1		12.15	13.526
1xy	7.69±0.1		7.69	6.487
2xx	48.7±0.4	25.9±0.4	37.3	35.915
2yy	−9.6±0.4	9.6±0.4	0.0	−1.564
3xx	4.3±0.2	0.4±0.2	2.4	2.042
3zz	−0.5±0.2	−3.7±0.2	−2.1	−0.05
3xy	2.3±0.4	3.6±0.2	2.95	2.871
4xx	−1.0 ±0.1		−1.0	−1.257
4yy	−0.22±0.03		−0.22	0.432
4yz	−0.03±0.1		−0.03	0.516
4xy	0.14±0.08		0.14	0.007

trons.

Figure 2 shows the phonon dispersion along the symmetry directions in $Fe_{0.5}Ti_{0.5}$ as calculated for the parameter set in Table III. There is practically no separation between optical- and acoustical-phonon bands. This can also be seen from the total [Fig. 3(a)] and the two partial [Fig. 3(b)] phonon densities of states $g(\nu)$. For comparison with other experiments it is useful to calculate the moments μ_n of the spectrum,

$$\mu_n = \frac{\int_0^\infty \nu^n g(\nu) d\nu}{\int_0^\infty g(\nu) d\nu} . \tag{5}$$

Since the μ_n span a very wide range, it is convenient to define a distribution of Debye "cutoff" frequencies ν_n defined by

$$\nu_n = \left[\frac{n+3}{3} \mu_n \right]^{1/n} \tag{6}$$

for $n \neq 0$, $n > -3$. For $n=0$ and -3 we have

$$\nu_0 = \exp\left[\frac{\frac{1}{3} + \int_0^\infty g(\nu) \ln \nu \, d\nu}{\int_0^\infty g(\nu) d\nu} \right] ,$$
$$\nu_{-3} = (k/h)\Theta_D(0\ \mathrm{K}) , \tag{7}$$

where h is the Planck constant, k is the Boltzman constant, and $\Theta_D(0\ \mathrm{K})$ is the specific-heat Debye temperature at 0 K. The Debye cutoff frequencies are shown in Fig. 4 as a function of n. The specific heat calculated from the phonon density of states of Fig. 3(a) is compared in Fig. 5 to measured values.[18] These are slightly lower than the calculated ones (2% on the average), indicating a Debye temperature which is about 10% higher than the calculated room-temperature value of 441 K. The calculated $\Theta_D(0\ \mathrm{K}) = 480$ K (calculated with the assumption of a temperature-independent phonon density of states) is also decidedly lower than $\Theta_D(0\ \mathrm{K})$ obtained from specific-heat measurements at low temperature[19–21] (495, 514, and 520 K, respectively). The discrepancy is not unexpected, however. Firstly, both shear moduli obtained from the Born–von Kármán fit are slightly too low compared to the measured single-crystal values (see Table III). Secondly, the Debye temperature at 0 K is determined by the elastic constants at this temperature, which in most cases are several percent harder than the room-temperature values. If our measured values (Table II) are extrapolated down to 0 K with the thermoelastic coefficients $T_{11} = -0.19 \times 10^{-3}$ K^{-1}, $T_{12} = 0.04 \times 10^{-3}$ K^{-1}, and $T_{44} = -0.21 \times 10^{-3}$ K^{-1} given by Liebertz *et al.*,[8] one gets $T_D = 508$ K

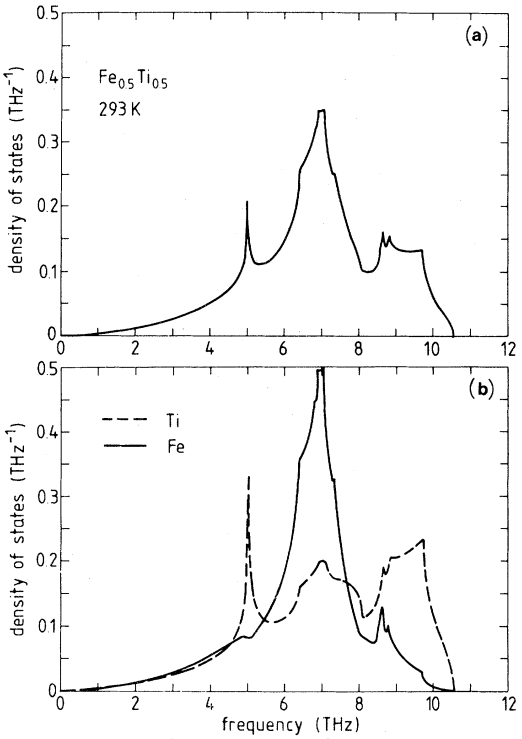

FIG. 3. Total (a) and partial (b) (Fe continuous line, Ti broken line) phonon densities of states in $Fe_{0.5}Ti_{0.5}$.

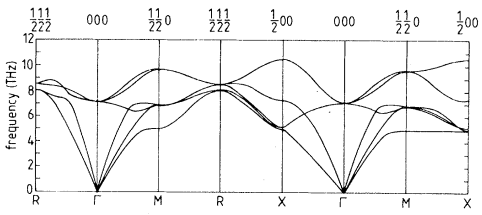

FIG. 2. Phonon dispersion along the symmetry directions in $Fe_{0.5}Ti_{0.5}$ at room temperature determined from polycrystal scattering.

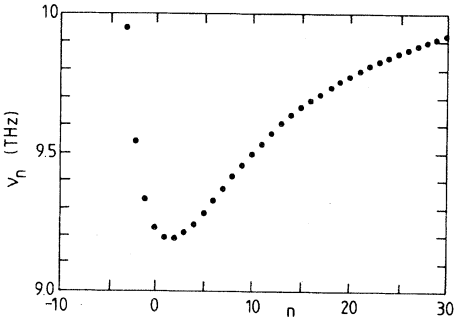

FIG. 4. Debye cutoff frequencies ν_n as a function of n for $Fe_{0.5}Ti_{0.5}$.

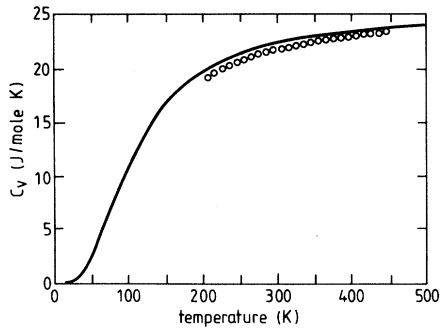

FIG. 5. Lattice contribution to the specific heat of $Fe_{0.5}Ti_{0.5}$ calculated with the force constants in Table III as a function of temperature (continuous line) and experimental values (Ref. 18) (open circles).

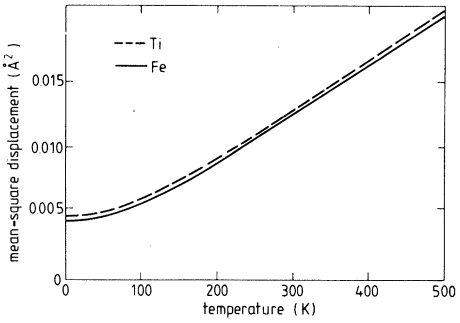

FIG. 6. Calculated mean-square displacements $\langle u^2 \rangle_{av}$ for Fe (continuous line) and Ti (broken line) in $Fe_{0.5}Ti_{0.5}$ as a function of temperature.

in good agreement with the low-temperature specific-heat data.

Figure 6 shows calculated mean-square displacements $\langle u^2 \rangle_{av}$ for Fe and Ti. They are nearly equal for both atoms. Obviously the heavier mass of the iron atom which would tend to give it a smaller mean-square displacement is compensated by the stronger binding of the titanium atom.

In conclusion, the phonon dispersion curves of $Fe_{0.5}Ti_{0.5}$ have been measured using two different neutron scattering methods. In the first, low-frequency phonons were measured conventionally with a small single crystal on a triple-axis spectrometer. From these phonons elastic constants could be determined. The phonons at higher frequencies were obtained with a newly developed method using a polycrystalline sample. $Fe_{0.5}Ti_{0.5}$ is the first substance with two atoms per unit cell measured by this method. As in the simpler cases studied before,[5] the evaluation showed that a a large number of force constants can be determined with surprising accuracy. On the other hand, the evaluation has also shown that ambiguities can appear, which can only be resolved by additional evidence. The force-constant set thus determined shows striking differences between nearest-neighbor Ti-Ti and Fe-Fe pairs, which can be explained qualitatively in terms of the bigger ionic radius of Ti. The averaged force constants correspond closely to those of chromium, which is isoelectronic with $Fe_{0.5}Ti_{0.5}$ and has a very similar band structure.

ACKNOWLEDGMENTS

Dr. E. Fisher (Argonne National Laboratory) kindly communicated to us his results on two longitudinal wave velocities in $Fe_{0.5}Ti_{0.5}$ and M. Beyss helped us to prepare the samples.

[1]R. Wiswall, in *Hydrogen in Metals II*, Vol. 29 of *Topics in Applied Physics*, edited by G. Alefeld and J. Völkl (Springer, Berlin, 1978), Chap. 5.
[2]J. Yamashita and S. Asano, Prog. Theor. Phys. 48, 2119 (1972).
[3]D. A. Papaconstantopoulos, Phys. Rev. B 11, 4801 (1975).
[4]G. N. Kamm, Phys. Rev. B 12, 3013 (1975).
[5]U. Buchenau, H. R. Schober, and R. Wagner, J. Phys. (Paris) 42, C6-395 (1981).
[6]J.-M. Welter, M. Beyss, and A. J. Singh (unpublished).
[7]E. Fisher (private communication).
[8]J. Liebertz, S. Stahr, and S. Haussühl, Krist. Tech. 15, 1257 (1980).
[9]W. Marshall and S. W. Lovesey, *Theory of Thermal Neutron Scattering* (Oxford University Press, Oxford, 1971), pp. 87–89.
[10]C. Stassis and J. Zarestky (private communication).
[11]R. A. Cowley, W. Cochran, B. N. Brockhouse, and A. D. B. Woods, Phys. Rev. 131, 1030 (1963).
[12]W. M. Shaw and L. D. Muhlestein, Phys. Rev. B 4, 969 (1971).
[13]W. Marshall and S. W. Lovesey, Ref. 9, p. 88, formula (4.88).
[14]W. Marshall and S. W. Lovesey, Ref. 9, p. 89, formula (4.89).
[15]V. F. Turchin, *Slow Neutrons* (Sivan, Jerusalem, 1965), p. 59ff.

[16]W. Marshall and S. W. Lovesey, Ref. 9, p. 95ff.
[17]K. Ikeda, Phys. Status Solidi B 62, 655 (1974).
[18]J.-M. Welter and Chr. Dieker (unpublished).
[19]E. A. Starke, Jr., C. H. Cheng, and P. A. Beck, Phys. Rev. 126, 1746 (1962).
[20]K. Ikeda, T. Nakamichi, and M. Yamamoto, J. Phys. Soc. Jpn. 37, 652 (1974).
[21]R. Hempelmann, D. Ohlendorf, and E. Wicke, in *Hydrides for Energy Storage, Geilo, Norway, 1977* (Pergamon, Oxford, 1978), p. 407.